XL CILAMCE
IBERO-LATIN AMERICAN CONGRESS ON COMPUTATIONAL METHODS IN ENGINEERING
NOVEMBER 11-14, 2019
Praiamar Natal Hotel & Convention
Natal, RN-BRAZIL

MATHEMATICAL MODELING, LINEAR CONTROL AND CONTACT DYNAMICS OF A UNDERWATER VEHICLE WITH 2 DEGREES OF FREEDOM

Eduardo dos Santos Sousa
André Fenili
eduardo.sousa@ufabc.edu.br
andre.fenili@ufabc.edu.br
Universidade Federal do ABC
Avenida dos Estados, nº5001, 09210-580, São Paulo / Santo André, Brasil

Abstract. This paper investigates the contact dynamics of a hybrid underwater vehicle operated remotely. In this first model, the vehicle has two degrees of freedom, executing the movement of submersion and rotation around it's center of mass. The main activity of such vehicle is to perform inspections on underwater and naval structures. For this, it is equipped with a set of motorized tracks. In this model, two points of contact will be considered along the length of the motorized tracks. Each of these points, when in contact, caracterizes a solution to the problem. The contact occurs on horizontal surface with complicity. To analyze this phenomenon will be using the Lagrange multipliers method to compute the contact force at each point of contact of the motorized tracks. In order to control the angular position of the vehicle, a control law will be proposed based on the LQR (Linear Quadratic Regulator) control methodology, the purpose of this control law is to provide that the two contact points established on the vehicle's motorized tracks will simultaneously contact or ensure that vehicle contacts the surface through one of these points.

Keywords: Underwater vehicle, Contact dynamics, Linear control

1 Introduction

Underwater activities have become increasingly intense in Brazil, in the areas related to the exploration of marine resources, biological research and aspects related to national security, has raised interest in the study and development of various types and models of small submersible vehicles [1].

A remotely operated submersible vehicle (ROV) is a small submersible mobile device, normally operated by a crew on board a ship. Being the North American and British navy the pioneers in the testing and development of such device, with the purpose of employing them in military activities [2] and [3].

Subsequently, given the great potential presented by the device, together with the interest and technological development of the device, the autonomous submersible vehicle (ASV) emerged as a robotic device driven through the water by a propulsion system, equipped with sensors and actuators, controlled by an embedded computer [4] and [5].

Due to the great economic and technological potential of autonomous and remotely operated submersible vehicles, their relevance becomes even greater in activities aimed at deepwater oil exploration and exploration data collection for the environment and marine biology, large floating or underwater structures, as well as missions to rescue victims and equipment lost in accidents [3] and [5].

1.1 Contact dynamics

As can be seen in [6] and [7] the collision between two bodies occurs in a very short time, during which the two bodies exert one on top of the other high amplitude forces.The force that appers normal the contact surfaces, due to the interaction between them is commonly described in the literature as impact force[8]

According to [7] there are two methods that can be used to investigate impact in dynamic systems, the discrete method and the continuous method. In the discrite method the main objective is to determine what happens to the system after the impact condition, in the continuous method, the main interest is to model the contact forces.

Most of the cases dealt with in the literature deal with systems without the restriction condition or with systems already in contact condition (restricted movement) the transition from the condition of free movement to restricted is not much approached in the literature, the transition analysis involves the study of the impact condition[6]

The study of the dynamics of the submersible vehicle in this work occurs through two conditions, free movement and restricted movement. The restriction condition applies when the vehicle is in contact with the contact surface through the mechanical tracks.

The objective of the mathematical model presented here in this paper is to describe and demonstrate the dynamics of free movement, restricted movement and the transition between this two conditions for an undewater vehicle and compute the contact force for simulated conditions.

The vehicle is equipped with actuator sensors that are of great importance to the full operation of the vehicle in it's work environment, so high-intensity impact forces can damage sensors and actuators, especially the mechanical track motors. In addition, another situation that should be avoided is the repetition of the transition condition of free and restricted movement, because according to [6] this causes an undesirable oscillatory behavior and may also cause severe damage to vehicle components.Given the conditions described, it is desired that the vehicle, when in contact with another object (performing inspection tasks for example), do not lose the touch.

2 Brief description of vehicle prototype

In this section will be briefly describe some mechanical properties of the studied vehicle and a brief description of the sensors and actuators equipped as illustrated by the following Fig.1.

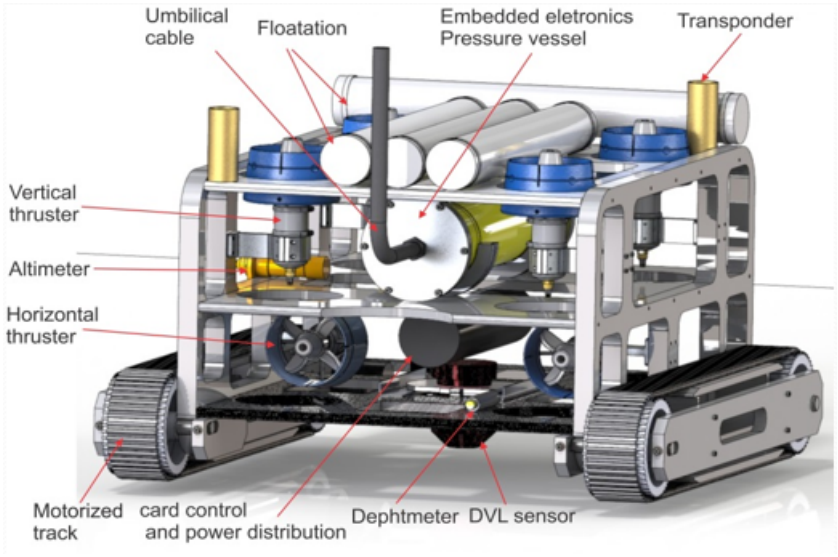

Figure 1. The HROV underwater vehicle

The hybrid remotely operated vehicle (HROV) prototype illustrated by Fig.1 was built at the Universidade Federal do ABC. The main activity of the vehicle is to perform ship hull inspections by means of ultrasound transducers to check plate thickness and for cracks. The vehicle is classified as a HROV due to the two modes of operation, freestyle and crawl. In the freestyle mode operation, the vehicle use six thrusters, four vertical and two horizontal for it's displacement through the water, for the crawl mode operation, the vehicle uses two motorized tracks for it's movement on the surface of the ship's hull [5] and [9].

2.1 Brief description of mechanical designer

The mechanical struture of HROV consist of polypropylene plates and is divided into two parts, upper and bottom. The upper part of the vehicle contains a floating, an acoustic positioning system compose by two transponders, a pressure vessel for control electronics and sensors, and four vertical thrusters.The bottom part of vehicle consists of two horizontal thrusters and two motorized mechanical tracks illustrated through Fig.1 [5] and [4]. The thrusters and motorized mechanical tracks are actuated by DC brushless eletric motors. Some navigation sensors are fixed on the structures of the vehicle and an umbilical cable is used for electric power supply and data transmission. Modular structural components allow HROV to be easily reconfigured in agreement with specifc tasks[9].

2.2 Brief description of sensors

The vehicle has the sensors system that provides the position and orientation of the vehicle with respect to an earth-fixed reference frame. The ultrasonic altimeter measures the distances between vehicle and the ship hull .The DVL-Doppler Velocity Log sonar provides the velocity of the vehicle in the surge, sway and heave directions, the vehicle poses a navigation instrument that contains attitude sensors to mensure the roll and picth angles and a compass to provide the heading of the vehicle. The navigation of the vehicle in the hull surface is based on information provides by camera, map of the hull and two transponders, the main task of the sensors system is to provide information for a robust estimation of position and velocity while combining information from different sensors using a stochatic sensors fusion algorithm [4] and [9]

3 Mathematical modeling

In this section, It will be describe the methodology employed to obtain the equations of motion of the vehicle under free and restricted motion conditions.Consider the following geometric representation of the problem, illustrated by Fig.2 below.

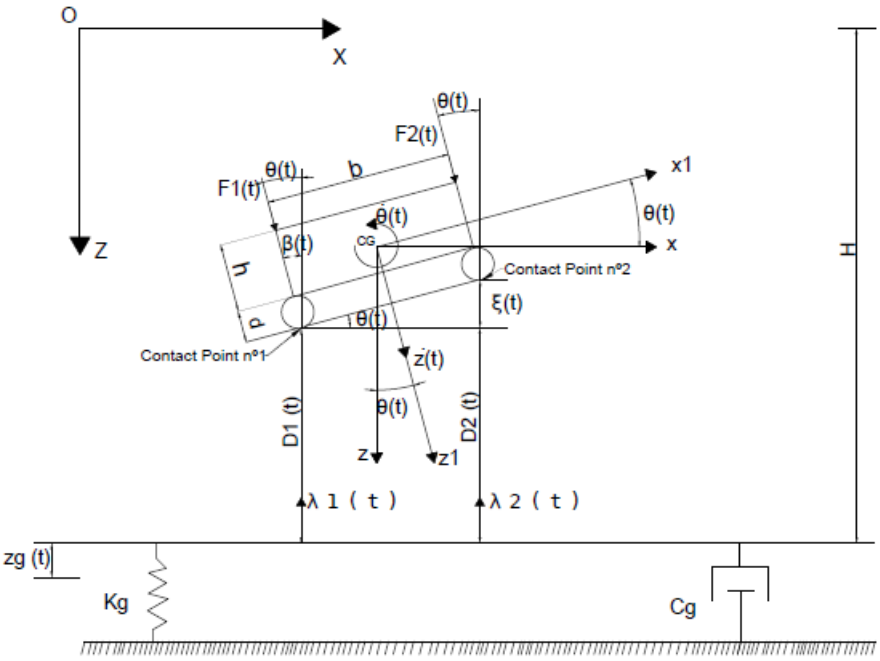

Figure 2. Geometric model of the problem

As mentioned earlier, in this model, the vehicle can travel in Z direction and rotate around it's center of mass, ie vehicle has two degrees of freedom, for this model, the displacement in the X direction will not be considered. To obtain the equations of motion, it will be considered that the mechanical track and the vehicle are only a rigid body, another simplification adopted is that the effects of quadratic and linear fluid drag on the vehicle will not be considered. Only the effect of the buoyant force applied to the respective center of buoyancy of the vehicle will be considered, which at this first moment is considered to coincide with the center of mass and the geometric center of the vehicle (CG).

The coordinates D_1 (t) and $D_2(t)$ indicate the distances from the vehicle contact points to the contact surface. K_G and C_G represent the contact surface stiffness and damping constant of the contact surface, $z_G(t)$ is the contact surface displacement coordinate, $z(t)$ coordinate indicates the displacement of the vehicle's center of mass. H indicates the total depth, the $\theta(t)$ coordinate indicates the rotation of the vehicle around its respective center of mass, $\lambda_1(t)$ and $\lambda_2(t)$ are the contact forces that arise during the vehicle's interaction with the surface, $F_1(t)$ and $F_2(t)$ are approximations of the thrust forces produced by the upper thrusters of the vehicle. Finally h represents the total height of the vehicle body, b the total length of the vehicle and the mechanical track, d the height of the mechanical track gears.

Note that X and Z are the axes of the surface inertial frame, x and z are the frame coordinates fixed on the vehicle body.

According to the geometrical model illustrated by Fig.3, the total kinetic energy of the vehicle can be described by means of the following equation:

$$T = \frac{1}{2}m\dot{z}(t)^2 + \frac{1}{2}I_{yy}\dot{\theta}(t)^2 \tag{1}$$

The first term of Eq. (1) refers to translation kinetic energy, and the second term to rotation kinetic energy, m being the total mass of the vehicle, I_{yy} the rotation inertia about the Y axis, $\dot{z}(t)$ the velocity driving direction Z and $\dot{\theta}(t)$ the angular speed of vehicle.

The total potential energy is defined by the following equation:

$$V = mgz - \rho g \nabla z \tag{2}$$

The first term of Eq. (2) refers to the potential energy and the second term the buoyancy force by the fluid, g being defined as gravitational acceleration, $z(t)$ the position of the center of mass of the vehicle, ρ the fluid density, ∇ the displaced volume of fluid.

After defining the expressions for kinetic and potential energy, the Lagrange equation for the vehicle is defined by the following equation.

$$L = T - V \tag{3}$$

Substituting the Eq. (1) and Eq. (2) into Eq. (3) results.

$$L = \frac{1}{2} m \dot{z}(t)^2 + \frac{1}{2} I_{yy} \dot{\theta}(t)^2 - mgz + \rho g \nabla z \tag{4}$$

The Lagrange equation described by Eq. (4) is almost complete as the constraint equations are still missing. To define the constraint equations of the problem, the geometric model illustrated by Fig .3 will be used, the variables $\beta(t)$ and $\xi(t)$ are defined by the following equations.

$$\beta(t) = \left(\frac{h}{2} + d\right) cos(\theta(t)) \tag{5}$$

$$\xi(t) = bsen(\theta(t)) \tag{6}$$

The variables described by Eq.(5) and Eq.(6) were used only to simplify the problem geometry illustrated by Fig.3 and by these equations, plus the illustration of Fig.3 can be defined constraint $D_1(t)$ and $D_2(t)$ as:

$$D_1(t) = H - \left[z(t) + \left(\frac{h}{2} + d\right) cos(\theta(t))\right] + z_G(t) \tag{7}$$

$$D_2(t) = H - \left[z(t) + \left(\frac{h}{2} + d\right) cos(\theta(t)) - bsen(\theta(t))\right] + z_G(t) \tag{8}$$

Now defining the constraint equations, the Eq.(4) can be rewrite by adding Lagrange multipliers and constraint equations as shown below.

$$\begin{aligned} L = \frac{1}{2} m \dot{z}(t)^2 + \frac{1}{2} I_{yy} \dot{\theta}(t)^2 - mgz(t) + \rho g \nabla z(t) \\ - \lambda_1(t) \left\{ H - \left[z(t) + \left(\frac{h}{2} + d\right) cos(\theta(t))\right] + z_G(t) \right\} \\ - \lambda_2(t) \left\{ H - \left[z(t) + \left(\frac{h}{2} + d\right) cos(\theta(t)) - bsen(\theta(t))\right] + z_G(t) \right\} \end{aligned} \tag{9}$$

To obtain the equations of motion, substitute Eq.(9) in the following equation given in [6].

$$\frac{d}{dt}\left(\frac{\partial L}{\partial \dot{q}_k}\right) - \frac{\partial L}{\partial q_k} = Q_k + \sum_{l=1}^{m} \lambda_l a_{lk} \tag{10}$$

Where q_k is the generalized coordinates of the vehicle and $\dot{q}_k$ the generalized velocity, Q_k is the work of generalized forces, which for this model will be the thrust force of the thruster, and $\sum_{l=1}^{m} \lambda_l a_{lk}$ as the bonding forces of the system, which are the contact forces of point 1 and point 2. Being l a quantity of Lagrange multipliers, a_{lk} the quantity of equations of bond. Note that λ now it will be considered as

a problem variable, and it should be derived Lagrange equation in relation to it. Substituting the Eq.(9) into Eq.(10) gives the following set of equations to be solve.

$$\frac{d}{dt}\left(\frac{\partial L}{\partial \dot{z}}\right) - \frac{\partial L}{\partial z} = F_1(t)cos(\theta(t)) + F_2(t)cos(\theta(t)) \tag{11}$$

$$\frac{d}{dt}\left(\frac{\partial L}{\partial \dot{\theta}}\right) - \frac{\partial L}{\partial \theta} = \frac{F_1(t)cos(\theta(t))b}{2} - \frac{F_2(t)cos(\theta(t))b}{2} \tag{12}$$

$$\frac{d}{dt}\left(\frac{\partial L}{\partial \dot{\lambda_1}}\right) - \frac{\partial L}{\partial \lambda_1} = 0 \tag{13}$$

$$\frac{d}{dt}\left(\frac{\partial L}{\partial \dot{\lambda_2}}\right) - \frac{\partial L}{\partial \lambda_2} = 0 \tag{14}$$

Solving for Eq.(11) gives the following equation.

$$m\ddot{z}(t) + mg - \rho g\nabla - \lambda_1(t) - \lambda_2(t) = F_1(t)cos(\theta(t)) + F_2(t)cos(\theta(t)) \tag{15}$$

Solving for Eq.(12) gives the following equation.

$$I_{yy}\ddot{\theta}(t) + \lambda_1(t)\left[\left(\frac{h}{2}+d\right)sen(\theta(t))\right] + \lambda_2(t)\left[\left(\frac{h}{2}+d\right)sen(\theta(t)) + bcos\left(\theta(t)\right)\right] = \frac{F_1(t)cos(\theta(t))b}{2} - \frac{F_2(t)cos(\theta(t))b}{2} \tag{16}$$

Solving for Eq.(13) and Eq.(14). Obtain the following equations respectively, defined as the relative distances between the contact points and the contact surface.

$$z_{rel1} = H - \left[z(t) + \left(\frac{h}{2}+d\right)cos(\theta(t))\right] + z_G(t) \tag{17}$$

$$z_{rel2} = H - \left[z(t) + \left(\frac{h}{2}+d\right)cos(\theta(t)) - bsen(\theta(t))\right] + z_G(t) \tag{18}$$

Now defining the equations of motion and the bond equations of the problem, the conditions of free movement and restricted movement for this proposed model can be establish. Note that there are three distinct solutions to the problem, being a solution only when a points come into contact individually or when both points come into contact condition simultaneously.

3.1 Free movement condition

In this section will define the conditions of free movement of the vehicle. For the free movement condition to be taken as true, the following condition must be established.

$$\begin{cases} z_{rel1}(t) \neq 0 & \lambda_1(t) = 0 \\ z_{rel2}(t) \neq 0 & \lambda_2(t) = 0 \end{cases} \tag{19}$$

Applying the conditions described by Eq.(19) to Eq.(15) and Eq.(16), the system dynamics under this condition will be represented by the following set of two nonlinear second order ordinary differential equations, as shown below.

$$m\ddot{z}(t) + mg - \rho g\nabla = F_1(t)cos(\theta(t)) + F_2(t)cos(\theta(t)) \tag{20}$$

$$I_{yy}\ddot{\theta}(t) = \frac{F_1(t)cos(\theta(t))b}{2} - \frac{F_2(t)cos(\theta(t))b}{2} \tag{21}$$

3.2 Movement restriction condition only through contact point number one

For the contact condition only by contact point number one to be taken as true, the following condition must be established.

$$\begin{cases} z_{rel1}(t) = 0 & \lambda_1(t) < 0 \\ z_{rel2}(t) \neq 0 & \lambda_2(t) = 0 \end{cases} \tag{22}$$

Applying the conditions set out in Eq.(22) in Eq.(15) and Eq.(16) results in the following set of differential equations.

$$m\ddot{z}(t) + mg - \rho g \nabla - F_1(t)cos(\theta(t)) - F_2(t)cos(\theta(t)) = \lambda_1(t) \tag{23}$$

$$I_{yy}\ddot{\theta}(t) = \frac{F_1(t)cos(\theta(t))b}{2} - \frac{F_2(t)cos(\theta(t))b}{2} \tag{24}$$

$$C_G\dot{z}_G(t) + K_G z_G = -\lambda_1(t) \tag{25}$$

Note that for Eq.(16) the constraints established in equation will not be taken into account in Eq.(24), since the contact surface presented here does not restrict vehicle rotation when only supported by the contact point one and two individually. The Eq.(25) is an ordinary linear first order differential equation, which according to [10] and [6] this can be used to represent the contact surface dynamics. Note that, the contact surface inertia is not being taken into account, this condition may be valid if only if is considered that the mass of the contact surface is much larger than that of the vehicle.

In this contact condition, both vehicle and the contact surface will oscillate together (even for a short time).This means that, in this condition the vehicle loses a degree of freedom in the Z direction. To describe the system dynamics in this condition, the Eq. (23) and Eq. (25) will be equated thus forming the following equation.

$$m\ddot{z}(t) + C_G\dot{z}_G(t) + K_G z_G + mg - \rho g \nabla - F_1(t)cos(\theta(t)) - F_2(t)cos(\theta(t)) = 0 \tag{26}$$

The Eq.(26) is a nonlinear, second order ordinary differential equation, which describes the system behavior in the contact condition through contact point one. Note that it is described as a function of contact surface and vehicle coordinates. To rewrite the Eq.(26) as a function of only the contact surface or vehicle coordinates, the Eq.(17) will be used, since in this contact condition $z_{rel1} = 0$ and its time derivative $\dot{z}_{rel1} = 0$ and thus the following relations for this contact condition is describe below.

$$\dot{z}_G = \dot{z}(t) - \left(\frac{h}{2} + d\right) sen(\theta(t))\dot{\theta}(t) \tag{27}$$

$$z_G = -H + \left[z(t) + \left(\frac{h}{2} + d\right) cos(\theta(t))\right] \tag{28}$$

Finally, substituting Eq.(27) and Eq.(28) in Eq.(26) can describe the system dynamics in this contact condition through the set of two nonlinear second order ordinary differential equations, shown below.

$$\begin{aligned} m\ddot{z}(t) + C_G \left[\dot{z}(t) - \left(\frac{h}{2} + d\right) sen(\theta(t))\dot{\theta}(t)\right] \\ + K_G \left\{-H + \left[z(t) + \left(\frac{h}{2} + d\right) cos(\theta(t))\right]\right\} \\ + mg - \rho g \nabla - F_1(t)cos(\theta(t)) - F_2(t)cos(\theta(t)) = 0 \end{aligned} \tag{29}$$

$$I_{yy}\ddot{\theta}(t) = \frac{F_1(t)cos(\theta(t))b}{2} - \frac{F_2(t)cos(\theta(t))b}{2} \tag{30}$$

3.3 Movement restriction condition only through contact point number two

For the contact condition only by contact point two to be taken as true, the following condition must be established.

$$\begin{cases} z_{rel1}(t) \neq 0 & \lambda_1(t) = 0 \\ z_{rel2}(t) = 0 & \lambda_2(t) < 0 \end{cases} \tag{31}$$

Applying the conditions set out in Eq.(31) in Eq.(15) and Eq.(16) results in the following set of differential equations.

$$m\ddot{z}(t) + mg - \rho g \nabla - F_1(t)cos(\theta(t)) - F_2(t)cos(\theta(t)) = \lambda_2(t) \tag{32}$$

$$I_{yy}\ddot{\theta}(t) = \frac{F_1(t)cos(\theta(t))b}{2} - \frac{F_2(t)cos(\theta(t))b}{2} \tag{33}$$

$$C_G\dot{z}_G(t) + K_G z_G = -\lambda_2(t) \tag{34}$$

The same conditions established for the contact condition for point one can be applied for point two, so the Eq.(32) and Eq.(34) results in the same equation obtained in Eq.(26).

$$m\ddot{z}(t) + C_G\dot{z}_G(t) + K_G z_G + mg - \rho g \nabla - F_1(t)cos(\theta(t)) - F_2(t)cos(\theta(t)) = 0 \tag{35}$$

Analogously for the contact condition established for contact point number one, for contact point number two has $z_{rel2} = 0$ and $\dot{z}_{rel2} = 0$ and by these conditions, using Eq. (18) we obtain the following relations.

$$\dot{z}_G = \dot{z}(t) - \left(\frac{h}{2} + d\right) sen(\theta(t))\dot{\theta}(t) - bcos(\theta(t))\dot{\theta}(t) \tag{36}$$

$$z_G = -H + z(t) + \left(\frac{h}{2} + d\right) cos(\theta(t)) - bsen(\theta(t)) \tag{37}$$

By substituting Eq.(36) and Eq.(37) in Eq.(35), the system dynamics in the contact condition through contact point number two can be described by a set of two nonlinear second order ordinary differential equations, described below.

$$\begin{aligned} m\ddot{z}(t) + C_G \left[\dot{z}(t) - \left(\frac{h}{2} + d\right) sen(\theta(t))\dot{\theta}(t) - bcos(\theta(t))\dot{\theta}(t)\right] \\ + K_G \left\{-H + \left[z(t) + \left(\frac{h}{2} + d\right) cos(\theta(t)) - bsen(\theta(t))\right]\right\} \\ + mg - \rho g \nabla - F_1(t)cos(\theta(t)) - F_2(t)cos(\theta(t)) = 0 \end{aligned} \tag{38}$$

$$I_{yy}\ddot{\theta}(t) = \frac{F_1(t)cos(\theta(t))b}{2} - \frac{F_2(t)cos(\theta(t))b}{2} \tag{39}$$

3.4 Condition of movement restriction through contact point number one and two

For the contact condition for both points to occur simultaneously, the following condition must be taken as true.

$$\begin{cases} z_{rel1}(t) = 0 & \lambda_1(t) < 0 \\ z_{rel2}(t) = 0 & \lambda_2(t) < 0 \end{cases} \tag{40}$$

Another requirement for this condition to be taken as true is that $\theta(t) = 0$ it imples that $z_{rel1}(t) = z_{rel2}(t)$. Therefore in this case, to describe the contact dynamics of the system, it can be use either Eq.(29) or Eq.(38), since $\theta(t) = 0$ both equations become identical,as shown below.

$$m\ddot{z}(t) + C_G\dot{z}(t) + K_G\left\{-H + \left[z(t) + \left(\frac{h}{2} + d\right)\right]\right\} + mg - \rho g\nabla - F_1(t) - F_2(t) = 0 \qquad (41)$$

In this condition, the dynamics of the system will be described only by the ordinary second order linear differential equation, as the two points are in contact, the vehicle can no longer rotate around the center mass, in this situation, unlike the others, the vehicle only has one degree of freedom.

3.5 Contact force

In this section we will define the expressions to compute the contact force in all cases previously discussed, for all cases the contact force can be obtained by Eq.(25) and Eq.(34).

3.5.1 Expression for contact force through contact point number 1

Using Eq.(25) and substituting Eq.(27) and Eq.(28) in Eq.(25) the expression to compute the contact force one will be defined as:

$$\lambda_1 = -C_G\left[\dot{z}(t) - \left(\frac{h}{2} + d\right) sen(\theta(t))\dot{\theta}(t)\right] - K_G\left[-H + z(t) + \left(\frac{h}{2} + d\right) cos(\theta(t))\right] \qquad (42)$$

3.5.2 Expression for contact force through contact point number 2

Using Eq.(34) and substituting Eq.(36) and Eq.(37) in Eq.(34) the expression to compute the contact force two will be defined as:

$$\lambda_2 = -C_G\left[\dot{z}(t) - \left(\frac{h}{2} + d\right) sen(\theta(t))\dot{\theta}(t) - bcos(\theta(t))\dot{\theta}(t)\right] - K_G\left[-H + z(t) + \left(\frac{h}{2} + d\right) cos(\theta(t)) - bsen(\theta(t))\right] \qquad (43)$$

3.5.3 Expression for contact force trough contact point number 1 and 2 simultaneously

In this situation, the contact force will be described by the sum of Eq.(42) and Eq.(43) divided by the number of contact as shown below, or it can be analyzed individually at each contact point.

$$\lambda = -\frac{1}{2}C_G\left\{\left[\left(\dot{z}(t) - \left(\frac{h}{2} + d\right) sen(\theta(t))\dot{\theta}(t) - bcos(\theta(t))\dot{\theta}(t)\right) + \left(\dot{z}(t) - \left(\frac{h}{2} + d\right) sen(\theta(t))\dot{\theta}(t)\right)\right]\right\} -\frac{1}{2}K_G\left\{\left[\left(-H + z(t) + \left(\frac{h}{2} + d\right) cos(\theta(t)) - bsen(\theta(t))\right) + \left(-H + z(t) + \left(\frac{h}{2} + d\right) cos(\theta(t))\right)\right]\right\} \qquad (44)$$

4 Quadratic linear optimal control

In this section it will be present the control law employed in the proposed mathematical model. Recalling that the purpose of the control law applied to this model will be to control the submersion

speed of the vehicle, with the purpose of attenuating the initial impact force on the mechanical track, and to control the angular position of the vehicle so that it comes in contact with the vehicle mechanical track.

According to [11] and [12] the application of LQR is desired when it is required that the output value of a given system reaches a desired value with the minimum control energy, minimizing a quadratic performance index described by the following equation.

$$J = \frac{1}{2}\left[\mathbf{x}(t_f)^T \mathbf{H}(t_f)\mathbf{x}(t_f)\right] + \frac{1}{2}\int_{t_0}^{t_f} \left\{\mathbf{x}(t)^T \mathbf{Q}(t)\mathbf{x}(t) + \mathbf{u}(t)^T \mathbf{R}(t)\mathbf{u}(t)\right\} dt \tag{45}$$

Where $\mathbf{H}(t_f)$ is the terminal cost weighted matrix, $\mathbf{Q}(t)$ is the error weighted matrix, being positive semidefinite, $\mathbf{R}(t)$ is the control weighted matrix and it should be positive definite, $\mathbf{x}(t)$ the state vector and $\mathbf{u}(t)$ the control vector.

4.1 State-space format model

In this section, it will be present the free-motion equations of the system in space-state format, according to the equation presented below as shown in [13].

$$\dot{\mathbf{x}}(t) = \mathbf{A}(t)\mathbf{x}(t) + \mathbf{B}(t)\mathbf{u}(t) + \mathbf{C}(t) \tag{46}$$

Where $\mathbf{A}(t)$ is the state matrix, $\mathbf{B}(t)$ is the control matrix, and $\mathbf{C}(t)$ is the matrix of terms that neither multiply the states nor the control, the Eq.(45) is defined in the literature as inhomogeneous LQR, applied to this model because of its presence of the gravity and buoyancy terms that do not multiply the state vector nor the control vector.

The Eq.(20) and Eq.(21) are nonlinear second-order differential equations, and describe the dynamics of the vehicle in the free-motion condition; however, to rewrite them in the described matrix format of Eq.(46), only small angular displacements and low linear and angular velocities will be considered, simplifying the $\cos(\theta(t)) \approx 1$ term of the equations. This approach can be valid because, according to [5], [9] and [4] the maximum travel speed of the vehicle is 1 meter per second. Rewriting Eq. (20) and Eq. (21) as Eq. (46).

$$\begin{bmatrix} \dot{x}_1(t) \\ \dot{x}_2(t) \\ \dot{x}_3(t) \\ \dot{x}_4(t) \end{bmatrix} = \begin{bmatrix} 0 & 1 & 0 & 0 \\ 0 & 0 & 0 & 0 \\ 0 & 0 & 0 & 1 \\ 0 & 0 & 0 & 0 \end{bmatrix} \begin{bmatrix} x_1(t) \\ x_2(t) \\ x_3(t) \\ x_4(t) \end{bmatrix} + \begin{bmatrix} 0 & 0 \\ \frac{1}{m} & \frac{1}{m} \\ 0 & 0 \\ \frac{b}{I_{yy}} & -\frac{b}{I_{yy}} \end{bmatrix} \begin{bmatrix} u_1(t) \\ u_2(t) \end{bmatrix} + \begin{bmatrix} 0 \\ g - \frac{\rho g \nabla}{m} \\ 0 \\ 0 \end{bmatrix} \tag{47}$$

Where $\dot{x}_1(t) = \dot{z}(t)$; $\dot{x}_2(t) = \ddot{z}(t)$; $\dot{x}_3(t) = \dot{\theta}(t)$; $\dot{x}_4(t) = \ddot{\theta}(t)$; $u_1(t) = F_1(t)$ and $u_2(t) = F_2(t)$

4.2 Linear controllability

To check the controllability of the system, Kalman's linear controllability criterion will be employed using the through the equation.

$$rank\left\{\mathbf{B}\vdots\mathbf{A}^1\mathbf{B}\vdots\mathbf{A}^2\mathbf{B}\vdots\cdots\vdots\mathbf{A}^{n-1}\mathbf{B}\right\} = n \tag{48}$$

Using matrices $\mathbf{A}(t)$ and $\mathbf{B}(t)$ in Eq. (48), it is verified that the controllability matrix rank is 4, that is, the system is completely controllable.

4.3 Inhomogeneous LQR optimal control law

The optimal control law for non-homogeneous LQR according to [14] and [13] can be defined as:

$$\mathbf{u}(t) = -\mathbf{R}^{-1}(t)\mathbf{B}^T(t)\mathbf{P}(t)\mathbf{x}(t) - \mathbf{R}^{-1}(t)\mathbf{B}^T(t)\mathbf{S}(t) \tag{49}$$

As described above, the main purpose of the control law described by Eq. (49) is to control the angular position of the vehicle, so that the contact condition always occurs through the mechanical tracks contact points, and to control the speed of submersion to such that this speed control promotes attenuation in the amplitude of the initial contact force. So basically, given any initial angular position for the vehicle, this control law has to be able to adjust the angular position of the vehicle until it reaches the desired value (θ_{ref}), the same condition is true for the submersion speed, given an initial sinks velocity, the control law must be able to adjust this submersion speed to the desired value $(\dot{z}_{rel})$ so that the vehicle sinks to the desired constant speed.

According to [14] to apply the tracking condition to the LQR, simply perform the following change in Eq.(49)

$$\mathbf{u}(t) = -\mathbf{R}^{-1}(t)\mathbf{B}^T(t)\mathbf{P}(t)(\mathbf{x}(t) - \mathbf{x}_{ref}(t)) - \mathbf{R}^{-1}(t)\mathbf{B}^T(t)\mathbf{S}(t) \tag{50}$$

Where $\mathbf{P}(t)$ is obtained by the solution of the Riccati matrix differential equation, and $\mathbf{S}(t)$ the auxiliary matrix differential equation provided by inhomogeneous terms, both equations are defined as.

$$\dot{\mathbf{P}}(t) = -\mathbf{P}(t)\mathbf{A}(t) - \mathbf{A}(t)^T\mathbf{P}(t) + \mathbf{P}(t)\mathbf{B}(t)\mathbf{R}^{-1}(t)\mathbf{B}^T(t)\mathbf{P}(t) - \mathbf{Q}(t) \tag{51}$$

$$\dot{\mathbf{S}}(t) = -\left(\mathbf{A}^T(t) - \mathbf{P}(t)\mathbf{B}(t)\mathbf{R}^{-1}(t)\mathbf{B}^T(t)\right)\mathbf{S}(t) - \mathbf{P}(t)\mathbf{C}(t) \tag{52}$$

In this case, as an infinite end time problem will be solved, the solutions of the equations can be obtained by the following algebraic equations, according to [13].

$$\bar{\mathbf{P}}(t) = -\bar{\mathbf{P}}(t)\mathbf{A}(t) - \mathbf{A}(t)^T\bar{\mathbf{P}}(t) + \bar{\mathbf{P}}(t)\mathbf{B}(t)\mathbf{R}^{-1}(t)\mathbf{B}^T(t)\bar{\mathbf{P}}(t) - \mathbf{Q}(t) \tag{53}$$

$$\bar{\mathbf{S}}(t) = -\left(\mathbf{A}^T(t) - \bar{\mathbf{P}}(t)\mathbf{B}(t)\mathbf{R}^{-1}(t)\mathbf{B}^T(t)\right)\bar{\mathbf{S}}(t) - \bar{\mathbf{S}}(t)\mathbf{C}(t) \tag{54}$$

With the following boundary condition $\bar{\mathbf{P}}(t_f \to \infty) = 0$ and $\bar{\mathbf{S}}(t_f \to \infty) = 0$ and and the quadratic index performance reduced to Eq.(55), as shown in[11].

$$J = \frac{1}{2}\int_{t_0}^{\infty}\left\{\mathbf{x}(t)^T\mathbf{Q}(t)\mathbf{x}(t) + \mathbf{u}(t)^T\mathbf{R}(t)\mathbf{u}(t)\right\}dt \tag{55}$$

5 Numerical simulation

This section describes the parameters used to perform numerical simulations and describe what will be analyze in each one. Our main goal is through these simulations is to demonstrate the system dynamics in the restricted movement condition and free movement condition. The Table1 below shows the constant parameters used in the three simulation that will be presented.

Simulation Parameters	Unit of Measurement (SI)
Vehicle mass (m)	140Kg
Moment of inertia (I_{yy})	19.7907 Kgm^2
Total depth (H)	15 m
Vehicle height (h)	0.705 m
Vehicle length (b)	1.076 m
Track Diameter (d)	0.3 m
Contact Surface Stiffness Coefficient (K_G)	5000 $\frac{N}{m}$
Contact Surface Damping Coefficent (C_G)	250 $\frac{Ns}{m}$
Fluid Density (ρ)	1000 $\frac{Kg}{m^3}$
Gravitational Acceleration Constant (g)	10 $\frac{m}{s^2}$
Vehicle Displaced Fluid Volume (∇)	0.145 m^3

Table 1. Numerical simulation constant parameters

The numerical value of vehicle mass, moment of inertia and volume of displaced fluid were obtained in [5], the contact surface stiffness and damping coefficients were obtained in [10]. The matrices $\mathbf{Q}$ and $\mathbf{R}$ used for the simulation of the all cases are described below.

$$\mathbf{Q} = diag\left\{3000, 5000, 100, 1\right\}; \mathbf{R} = diag\left\{\frac{1}{4}; \frac{1}{4}\right\}$$

5.1 Numerical simulation: Case 1

In this simulation the objective is to represent the contact condition only through contact point number one.The main idea here is to represent, even if simply, a situation where for example the vehicle needs assume a necessary angular configuration before contacting the object to be inspected, after contact occurs, the thrusters will be switched off and the buoyancy force of the fluid will act on the vehicle. The following Table1 gives the initial conditions for the first simulation.

Initial Conditions	Unit of measures (SI)
Initial Condition for Vehicle Position (x_1)	5 m
Initial Condition for Vehicle Speed (x_2)	0.2 $\frac{m}{s}$
Reference Speed (x_{2ref})	0.5 $\frac{m}{s}$
Initial Condition for Vehicle Angular Position (x_3)	0 °
Angular position of reference (x_{3ref})	5 °
Initial Condition for Vehicle Angular Speed (x_4)	0 °/s
Initial Condition for Contact Surface Position (x_5)	0 m

Table 2. Initial conditions for the first simulation

As described earlier, in this simulation, it is desired to position the vehicle in an established angular

position (x_{3ref}) and control the submersion speed to achieve a desired speed (x_{2ref}). Note that values of $x_3(t) > 0$ means that the vehicle is rotating counterclockwise, and based on Fig.3, it can be seen that for this simulated condition only the contact point number one will be in contact condition.

5.2 Numerical simulation: Case 2

This simulation is very similar to the simulation case 1, however, for this case the contact point that will enter in contact condition will be only the point number 2 , in this case $x_{3ref} < 0$ this means that the vehicle will rotate clockwise. Similarly to simulation number one, the submersion speed of the vehicle will be controlled, but for this simulation the value of x_{2ref} will be increased, so that it can be verified what happens with the amplitude of the initial impact force.

The same parameters described in Table 1 will be used in this simulation. The changes will be described in the following Table 3.

Initial condition	Unit of measures (SI)
Initial Condition for Vehicle Position (x_1)	5 m
Initial Condition for Vehicle Speed (x_2)	0.2 $\frac{m}{s}$
Reference Speed (x_{2ref})	0.8 $\frac{m}{s}$
Initial Condition for Vehicle Angular Position (x_3)	0 °
Angular position of reference (x_{3ref})	-5 °
Initial Condition for Vehicle Angular Speed (x_4)	0 °/s
Initial Condition for Contact Surface Position (x_5)	0 m

Table 3. Initial condition for the second simulation

5.3 Numerical simulation: Case 3

Finally the last simulation aims to adjust the angular position such that the contact points number one and number two enter the contact condition simultaneously. This condition can be approximated to a situation where some external force generates angular momentum on the vehicle causing an angular rotation around the center of the vehicle's mass to assume nonzero values, and in turn the control has to adjust the angular position of the vehicle.The parameters for this simulation will be described through Table 4 below.

Initial condition	Unit of measures (SI)
Initial Condition for Vehicle Position (x_1)	3 m
Initial Condition for Vehicle Speed (x_2)	0.4 $\frac{m}{s}$
Reference Speed (x_{2ref})	0.8 $\frac{m}{s}$
Initial Condition for Vehicle Angular Position (x_3)	5 °
Angular Position of Reference (x_{3ref})	0 °
Initial Condition for Vehicle Angular Speed(x_4)	0.3 °/s
Initial Condition for Contact Surface Position (x_5)	0 m

Table 4. Initial condition for second simulation

6 Results

In this section we will present the results of the numerical simulations and then the discussion of the results obtained.

6.1 Results of the case one

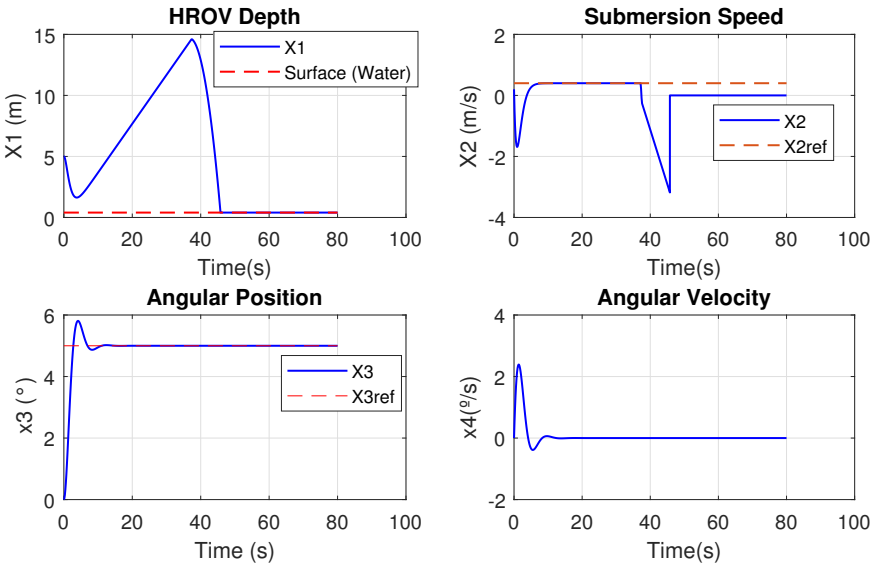

Figure 3. HROV states first simulation

Through Fig.3 it is possible to verify that states $x_2(t)$ and $x_3(t)$ reached the values $x_{2ref}(t)$ and $x_{3ref}(t)$. By means of the graph of state $x_2(t)$, it is possible to observe that the magnitude goes to zero and soon after changes of signal, this happened due to the contact condition has occurred and after happening after the vehicle loses the contact with the contact surface it can be verified by means of the state x_1 that it returns to the surface, that is, the change of sign of magnitude $x_2(t)$ describes the change of direction in the movement of the vehicle.

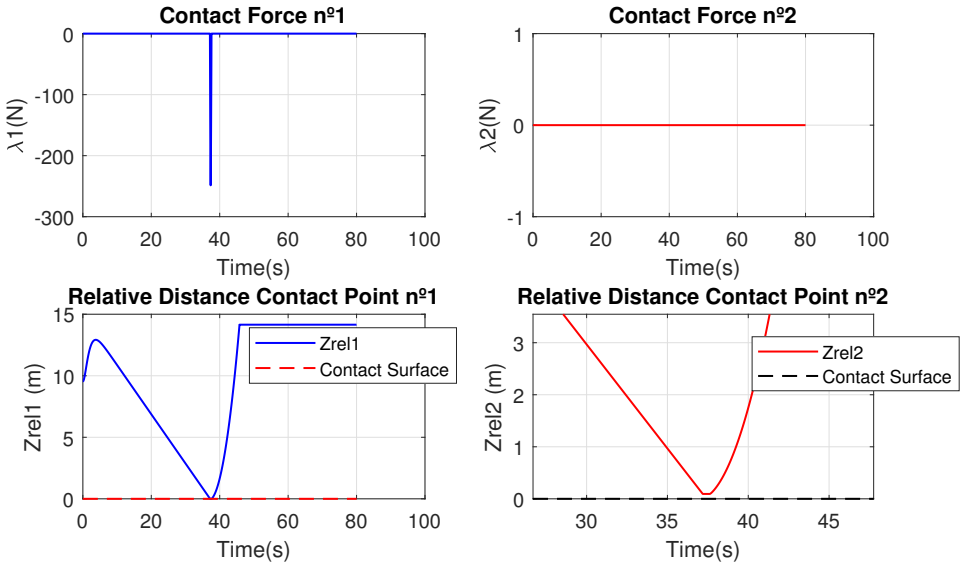

Figure 4. Contact force and relative distance

Through Fig.4, it is possible to verify that the vehicle has entered the restricted movement condition only through the contact point one, because $z_{rel1}(t) = 0$ and $z_{rel2}(t) \neq 0$. Soon after it can be seen that the relative distance $z_{rel1}(t)$ is increasing, ie the vehicle is moving away from the contact surface, it is also possible to see that only the contact force one shows up and it's magnitude.

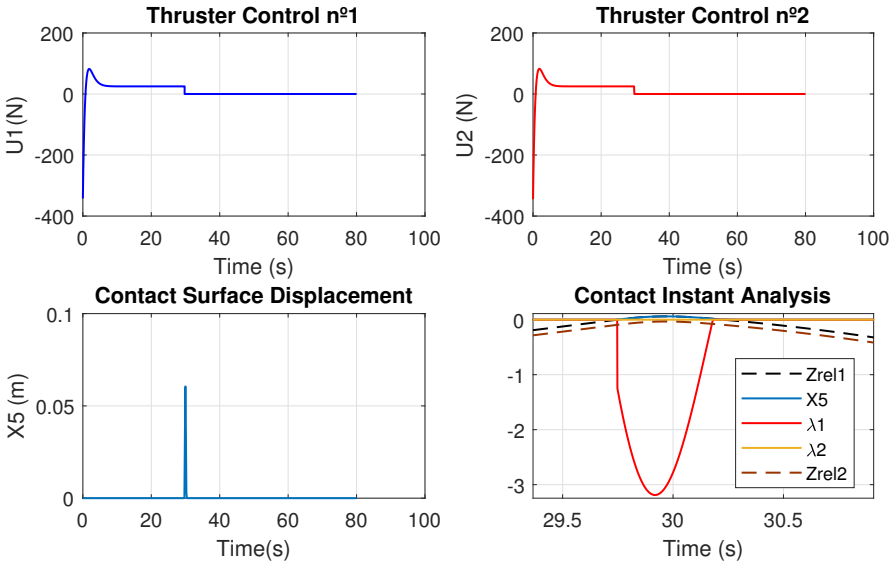

Figure 5. Control effort and contact surface displacement

Through Fig.5, it is possible to observe that the control effort when the contact condition occurs goes to zero, since in this model, the control of the thrust force to keep the vehicle in contact is not yet studied and it is also to check the exact time the contact occurred and its duration.

6.2 Results of the case two

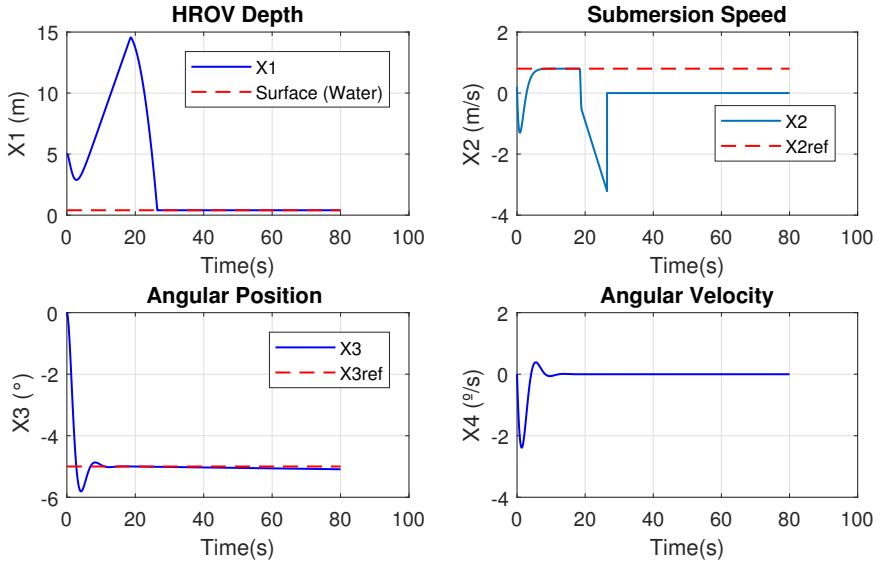

Figure 6. HROV states second simulation

Note that the results shown through Fig.6 is similar to the results shown through Fig.3. However, it can be seen that as the speed of submersion was higher than in case one, the impact happens a few minutes

earlier. The angular position and velocity had the same amplitude but negative due to the direction of rotation adopted.

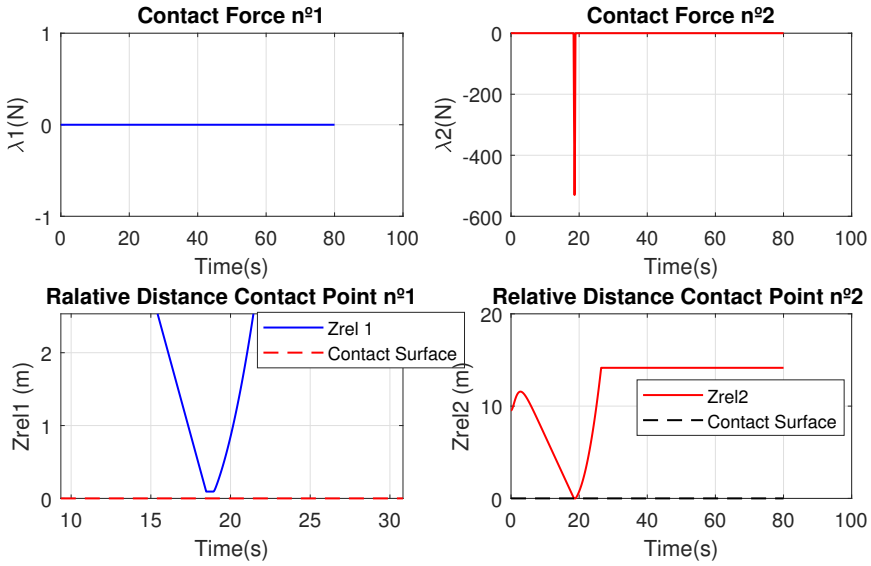

Figure 7. Contact force and relative distance second simulation

The result presented through Fig.7, it is possible to verify that the result is similar to the one presented in Fig.4, it can be verified that the amplitude of the contact force of point two is slightly larger, when compared to the contact force of point one illustrated in Fig .4, due to increased submersion speed.

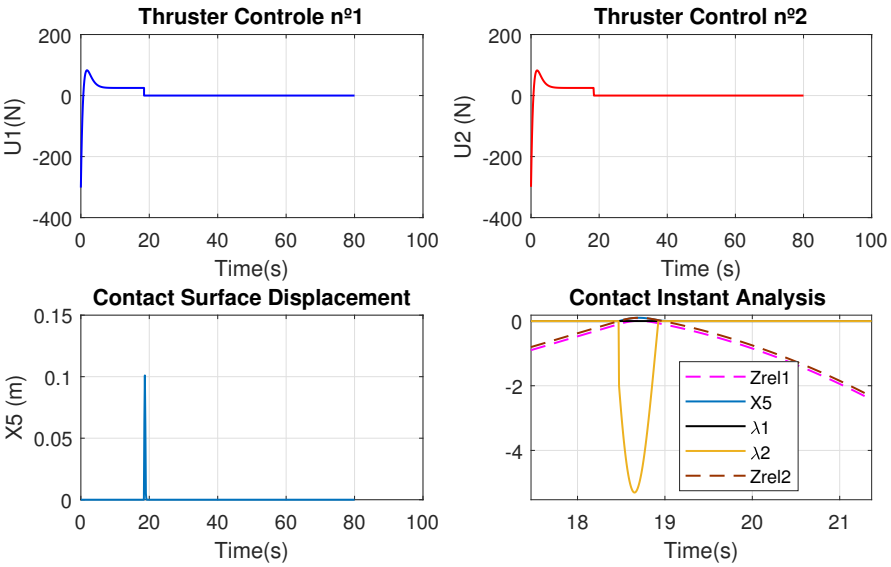

Figure 8. Control effort and contact surface displaced second simulation

In Fig.8 it is possible to verify that the amplitude of the contact surface displacement was greater when compared to the results presented in Fig.5, because the contact force amplitude has increased.

6.3 Results of the case three

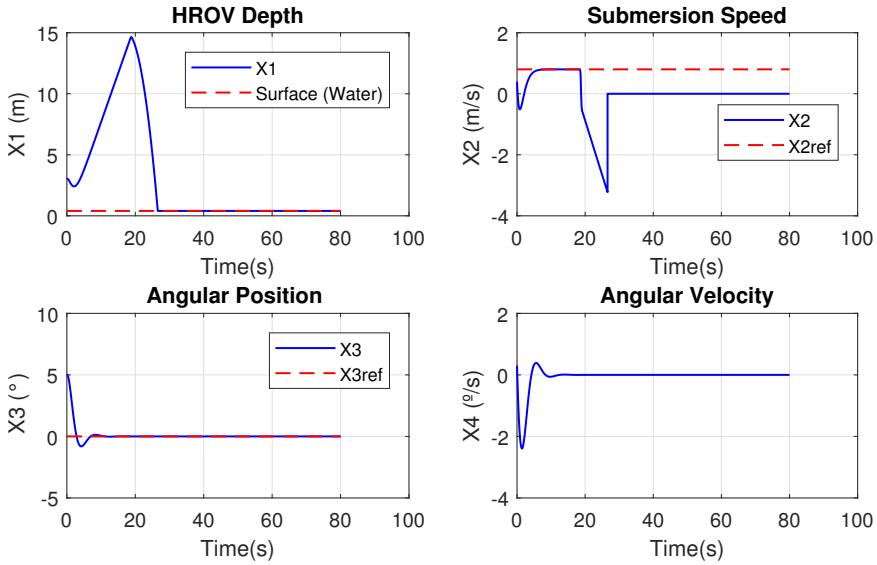

Figure 9. HROV states third simulation

The same result seen through Fig.6 can be seen in Fig.9, the only difference is in the angular position due to the change in the reference angle (x_{3ref}).

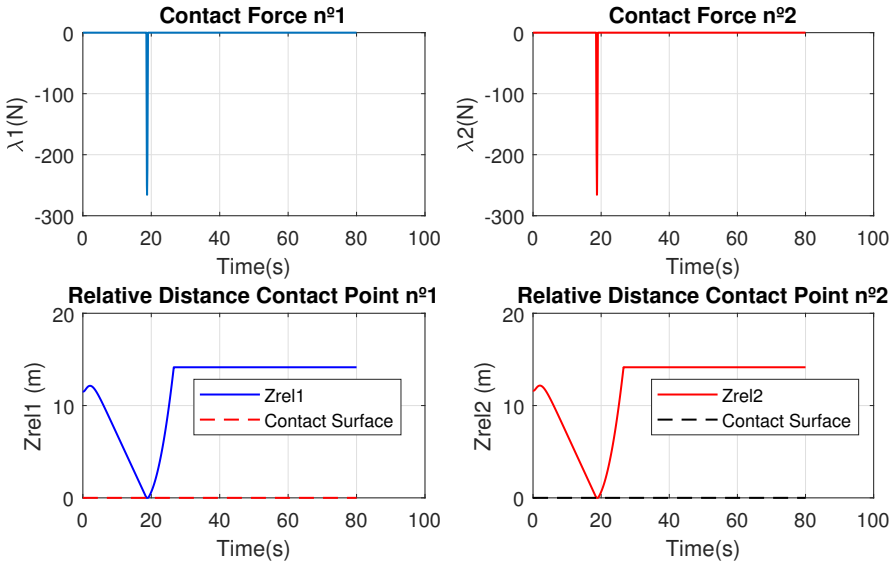

Figure 10. Contact force and relative distance third simulation

In this case, unlike the previous ones, it is possible to verify through Fig.10, the impact force on both contact points at the same time, and the contact force amplitude was computed with half of the contact force of point two, seen in Fig.7. Note that the contact forces have been demonstrated individually, and the total force is given by the sum of $\lambda_1(t)$ and $\lambda_2(t)$

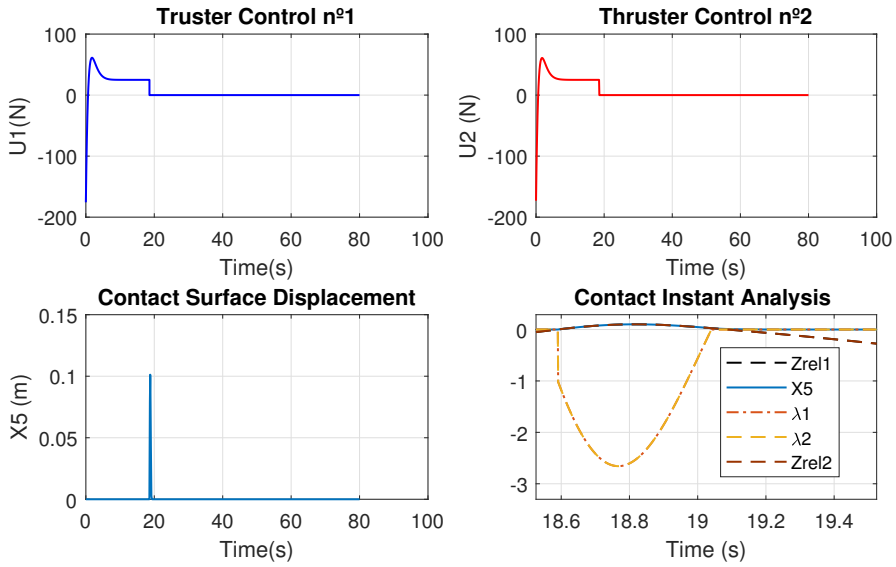

Figure 11. Control effort and contact surface displaced thirt simulation

Through Fig.10 it is possible to verify that there were no major changes when compared to Fig.8. Except in the figure that illustrates the moment of contact, where it can be seen the presence of contact force one and two simultaneously and the reduction of the amplitude of the forces of contact.

7 Conclusion

The mathematical model presented in this paper is a simplified version of the real system, since some important variations were not taken into account in the system modeling aspect. Even with the simplifications applied, it was possible to represent some real aspects of vehicle dynamics, such as the buoyant force that tends to keep the vehicle out of contact. By applying the submersion speed control, it was possible to verify and compare the attenuation of the initial contact force, which is interesting for the problem, since large amplitudes of this force can damage track components such as other actuators and vehicle sensors. Finally, this model studied in this paper, allowed the analysis and understanding of aspects that will be further developed and worked on, such as fluid parameters that influence vehicle dynamics, as well as the use of vehicle control force to ensure that the vehicle remains in contact condition.

References

[1] Luque, J. C. C., 2012. *Identificação e Controle de um Veículo Submersível Autônomo Sub-Atuado*. PhD thesis, Escola Politécnica de São Paulo. 1

[2] Hernández, W. P., 2012. Modelagem dinâmica de um robô submarino semi-autônomo (tipo rov) para inspeção de risers. Master's thesis, Universidade Federal do Rio de Janeiro. 1

[3] Wynn, R. B., Huvenne, V. A., Bas, T. P. L., Murton, B. J., Connelly, D. P., Bett, B. J., Ruhl, H. A., Morris, K. J., Peakall, J., Parsons, D. R., Sumner, E. J., Darby, S. E., Dorrell, R. M., & Hunt, J. E., 2014. Autonomous underwater vehicles (AUVs): Their past, present and future contributions to the advancement of marine geoscience. *Marine Geology*, vol. 352, pp. 451–468. 1

[4] Ferreira, C. Z., 2016. Sistema de controle de seguimento de trajetória de veículo robótico de inspenção de estrtuturas submarinas. Master's thesis, Universidade Federal do ABC. 1, 2.1, 2.2, 4.1

[5] Vicuña, P. R. B., 2016. Modelagem matemática e controle não linear de um veículo submersível operado de forma remota. Master's thesis, Universidade Federal do ABC, Santo André. 1, 2, 2.1, 4.1, 5

[6] Fenili, A. & Shäfer, B., 2007. Contact dynamics investigation. Post doctorate report, Institute of Robotics and Mechatronics Oberpfaffenhofen,Germany. 1.1, 3, 3.2

[7] Barragam, V. P., 2018. Formulação de complementaridade para dinâmica de contato de um manipulador robótico aerospacial. Master's thesis, Instituto Tecnológico de Aeronáutica. 1.1

[8] Beer, F. J., Johnston, J. E., & Mazurek, D., 2012. *Vector Mechanics for Engineers: Statics and Dynamics*. MCGRAW HILL BOOK CO. 1.1

[9] Ferreira, C. Z., Conte, G. Y. C., Avila, J. P. J., Pereira, R. C., & Ribeiro, T. M. C., 2014. Underwater robotic vehicle for ship hull inspection: Control system architecture. In *ABCM Symposium Series in Mechatronics-Vol.6*. ABCM. 2, 2.1, 2.2, 4.1

[10] Bibalan, P. T. & Featherstone, R., 2009. A study of soft contact models in simulink. In *Australasian Conference on Robotics and Automation*. 3.2, 5

[11] Naidu, D. S., 2002. *Optimal Control Systems*. CRC Press. 4, 4.3

[12] Kirk, D. E., 2004. *Optimal Control Theory*. Dover Publications Inc. 4

[13] Hampton, R. D., Knospe, C. R., & Townsend, M. A., 1996. A practical solution to the deterministic nonhomogeneous LQR problem. *Journal of Dynamic Systems, Measurement, and Control*, vol. 118, n. 2, pp. 354. 4.1, 4.3, 4.3

[14] Radhakant, P., 2018. Linear quadratic regulator (lqr)-ii. Indian Institute of Science- Bangalore. https://nptel.ac.in/courses/101108057/downloads/Lecture-11.pdf accessed on 07/12/2018 at 8:00 pm. 4.3, 4.3